



Next generation tools for high-throughput promoter and expression analysis employing single-copy knock-ins at the *Hprt1* locus

G.S. Yang^{a,1}, K.G. Banks^{b,1}, R.J. Bonaguro^b, G. Wilson^a, L. Dreolini^a, C.N. de Leeuw^{b,d}, L. Liu^c, D.J. Swanson^{c,2}, D. Goldowitz^{c,2}, R.A. Holt^{a,e}, E.M. Simpson^{b,d,*}

^a Canada's Michael Smith Genome Sciences Centre, British Columbia Cancer Agency, Vancouver, British Columbia, Canada V5S 4Z6

^b Centre for Molecular Medicine and Therapeutics, Child and Family Research Institute, University of British Columbia, Vancouver, British Columbia, Canada V5Z 4H4

^c Department of Anatomy and Neurobiology, The University of Tennessee Health Science Center, Memphis, Tennessee 38163, USA

^d Department of Medical Genetics, University of British Columbia, Vancouver, British Columbia, Canada

^e Department of Psychiatry, University of British Columbia, Vancouver, British Columbia, Canada

ARTICLE INFO

Article history:

Received 1 May 2008

Accepted 17 September 2008

Available online 3 December 2008

Keywords:

Embryonic stem cells

Gene targeting

Vectors

Genomics

Hprt1

Knock-in

Mice

Promoter regions

Transgenic

ABSTRACT

We have engineered a set of useful tools that facilitate targeted single copy knock-in (KI) at the hypoxanthine guanine phosphoribosyl transferase 1 (*Hprt1*) locus. We employed fine scale mapping to delineate the precise breakpoint location at the *Hprt1*^{b-m3} locus allowing allele specific PCR assays to be established. Our suite of tools contains four targeting expression vectors and a complementing series of embryonic stem cell lines. Two of these vectors encode enhanced green fluorescent protein (EGFP) driven by the human cytomegalovirus immediate-early enhancer/modified chicken beta-actin (CAG) promoter, whereas the other two permit flexible combinations of a chosen promoter combined with a reporter and/or gene of choice. We have validated our tools as part of the Pleiades Promoter Project (<http://www.pleiades.org>), with the generation of brain-specific EGFP positive germline mouse strains.

© 2008 Elsevier Inc. All rights reserved.

Introduction

The transgenic mouse continues to play an important role in the study of human development, physiology, and disease. We have designed a collection of tools that facilitate single-copy knock-in at the selectable hypoxanthine guanine phosphoribosyl transferase 1 (*Hprt1*) locus in mouse embryonic stem cells (ESCs). Consistent levels of transgene expression and little to no phenotypic variability in mouse strains derived from knock-ins at this defined insertion site produce uniformity of results and do not require examination of large numbers of mouse strains [1]. This is in contrast to random insertion experiments, where the initial knock-in step is simpler, but often leads to undesirable effects such as uncontrolled copy number, variable

expression levels, variability in phenotype, and insertional mutagenesis, necessitating the characterization of multiple strains of mice [2–5]. The *Hprt1* tool set we describe here facilitates targeted insertion such that the difficulty of the knock-in is less of a consideration in experimental design.

The HPRT1 enzyme is important in the salvage of purines for biosynthesis of nucleotides, providing an alternate to the *de novo* nucleotide synthesis pathways. Specifically, HPRT1 catalyzes the conversion of hypoxanthine and guanine to the mononucleotides IMP and GMP, respectively [6–9]. The *Hprt1* locus, located on the X Chromosome (Chr), is 44 kb in size and comprised of 9 exons [9]. HPRT1 is ubiquitously expressed in all tissues, and the *Hprt1* locus is relatively neutral as a transgene docking site because the locus has minimal influence on transgene expression when driven by an exogenous promoter [1,2,10]. Although functional deletion of *HPRT1* in humans leads to Lesch–Nyhan syndrome (reviewed in [11]), only a mild phenotype is observed in the mouse knockout [12–14], but in the knock-in (KI) mouse the sequences typically introduced into the locus complements the gene and *Hprt1* is expressed. Thus, the locus is useful in mice for single-copy gene targeting. A spontaneous deletion occurring at the mouse *Hprt1* locus, *Hprt1*^{b-m3} [15], has been well characterized in embryonic stem cells and mice (E14TG2a, HM-1 and

* Corresponding author. Centre for Molecular Medicine and Therapeutics, Child and Family Research Institute, University of British Columbia, Vancouver, British Columbia, Canada V5Z 4H4. Fax: +1 604 875 3819.

E-mail address: simpson@cmmt.ubc.ca (E.M. Simpson).

¹ These authors contributed equally to this work.

² Current address: Centre for Molecular Medicine and Therapeutics, Child and Family Research Institute, and Department of Medical Genetics, University of British Columbia, Vancouver, British Columbia, Canada V5Z 4H4.

B6.129P2-*Hprt1*^{b-m3}/J), and can be targeted using plasmids [16–18] and much larger bacterial artificial chromosome (BAC) constructs [10]. This spontaneous deletion removes two essential exons from the 5' end of the *Hprt1* locus. Complementation of the locus by homologous recombination with KI vectors containing the two deleted exons [16] allows positive selection of recombinants. A large majority of selected clones are typically correctly targeted [19–21]. This is an important advantage over more standard positive–negative selection systems for targeting. The ability to select, both positively, with HAT (hypoxanthine, aminopterin, thymidine), and negatively, with 6-thioguanine, for targeting events at this locus establishes *Hprt1* as a valuable tool for transgenesis both *in vitro*, and *in vivo* [9,17]. The X Chr location of the *Hprt1* locus can be a concern given that single copy insertions in females are subject to random X-inactivation, which may result in mosaic expression of the transgene [10]. However, the X Chr location of the *Hprt1* locus can also be beneficial as all the daughters of a carrier father will have the transgene, thus reducing the need for genotyping.

We have advanced the existing *Hprt1* targeting and expression system [16] and developed more sophisticated tools, including expression vectors, embryonic stem cells (ESCs), and PCR assays, for mouse genome modification at this locus. A new vector, pEMS1306, has been designed to facilitate the single copy delivery of either a promoter driving EGFP and/or a gene of interest to the *Hprt1* locus. In our current application, different promoter constructs of interest are inserted into the multiple cloning site and used to drive expression of a downstream enhanced green fluorescent protein (EGFP) reporter.

We have also developed two series of new hybrid ESCs that show high germline competence. These ESCs are hemizygous for the *Hprt1*^{b-m3} spontaneous deletion and heterozygous or wild-type (WT) for *Gt(Rosa)26Sor^{tm1Sor}*, which serves as a *Cre* reporter and historical marker. As with the traditional E14TG2a ESC line, these ESCs have proven useful for making new transgenic strains by conventional microinjection. An additional benefit of these new ESC lines is the ability to use the co-culture technique to produce germline competent chimeras, which is not permissible using E14TG2a [21]. These vectors and ESCs have also enabled us to derive a new strain of mice carrying the human cytomegalovirus immediate-early enhancer/modified chicken beta-actin (CAG) promoter driving the EGFP tetracycline reporter from pEMS1306, knocked in to the *Hprt1*^{b-m3} locus. Moreover we have defined the exact boundaries of the spontaneous breakpoint at *Hprt1*^{b-m3} carried by E14TG2a and the mouse strain B6.129P2-*Hprt1*^{b-m3}, enabling us to design new specific PCR assays for this and the *Hprt1* WT alleles. We have also designed primers that are specific for the *HPRT1* complementary sequence (*HPRT1*-CS: human-to-mouse) at the *Hprt1* locus only after it is complemented by a targeting event.

Results

Multi-featured vectors enable and expand functionality of docking at the *Hprt1* locus

Two targeting vectors, pEMS1306 and pEMS1307 (Fig. 1), were developed to facilitate single copy insertion of transgenes targeted to the *Hprt1* locus. The backbone sequence of both vectors contains the homologous sequence required to target the *Hprt1* locus in mouse ESCs that contain the *Hprt1*^{b-m3} deleted allele. Proper integration of the vectors complements the structure and function of the *Hprt1* gene and allows positive selection of the recombinants. Our vectors encode a multiple cloning site (MCS) containing a total of five restriction sites, including the eight-cutters, *FseI* and *AscI*. These two rare restriction sites are less likely to be found within the promoter to be cloned allowing greater opportunity for directional cloning of promoter constructs with a wider range of sequence variability. The chosen promoter drives expression of a reporter gene that is an EGFP/tetracycline motif fusion. The tetracycline tag allows alternative

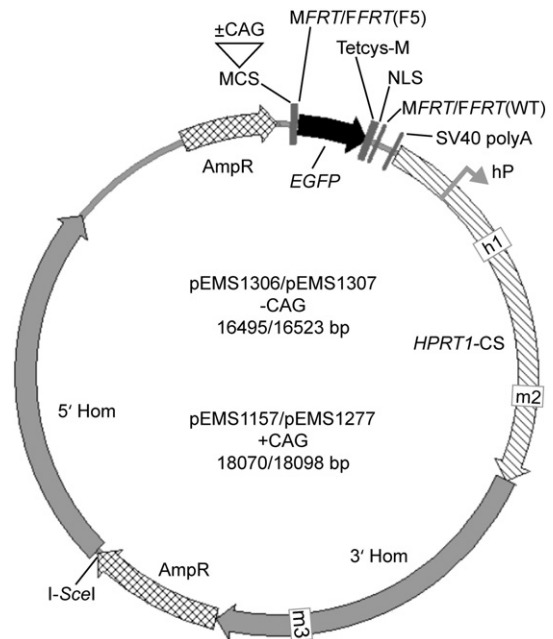


Fig. 1. Novel plasmid vectors facilitate single copy insertion at the *Hprt1* locus. pEMS1306/pEMS1307 (promoterless (-CAG)), and pEMS1157/pEMS1277 (+CAG) vectors containing *Hprt1* homology regions (5' Hom, 3' Hom, solid grey arrows), *HPRT1* complementary sequence (*HPRT1*-CS, slashed arrow), containing the human *HPRT1* promoter (hP), human exon 1 (h1), and mouse exon 2 (m2) and 3 (m3), multiple cloning site (MCS), minimal *FRT* (MFRT) and full *FRT* (FFRT) WT and F5 mutant sites, SV40 polyadenylation (SV40 polyA) site, nuclear localization signal (NLS), tetracycline motif (Tetcys-M), ampicillin resistance (AmpR, checked arrows), EGFP reporter (black arrow), and *I-SceI* linearization site.

detection by arsenical ligands [22]. In addition, the tetracycline-tagged EGFP marker is flanked by 5' mutant (F5), and 3' wild-type (WT) *FRT* sites, allowing Flp-recombination mediated cassette exchange (RMCE) [23] of the EGFP reporter with a preferred gene of choice. The pEMS1306 and pEMS1307 targeting vectors differ only in that pEMS1306 contains minimal *FRT* (MFRT), 34 bp, sites compared to the full *FRT* (FFRT), 48 bp, version in pEMS1307 [24]. This modification was driven by the successful use of *FFRTs* for RMCE in mouse ESCs [23,25,26]. There is also an upstream Kozak consensus sequence to increase the translation efficiency of the reporter gene in eukaryotic cells in addition to three copies of a nuclear localization signal (NLS) for increased translocation efficiency of the protein into the nucleus of the cells. An SV40 polyadenylation signal directs proper processing of the mRNA 3' end in both of these constructs.

Two additional constructs, pEMS1277, and pEM1277, were generated using the ubiquitously expressed human cytomegalovirus immediate-early enhancer/modified chicken beta-actin (CAG) promoter to test the functionality of the EGFP reporter in the pEMS1306 and pEMS1307 vector backbones. Four constructs, pEMS1306, pEMS1157, pEMS1307, and pEMS1277 were electroporated into mEMS1204 ESCs, and all of the constructs generated colonies upon HAT selection indicating proper homologous recombination and complementation of the *Hprt1*^{b-m3} locus. Colonies were picked for screening by PCR to confirm the presence of the transgene immediately upstream of the *Hprt1* locus. The high frequency (90–95%) of correct homologous recombination events we observe at the *Hprt1*^{b-m3} locus is similar to previously published data [10,16,18–20].

Enabling the utilization of the *Hprt1*^{b-m3} spontaneous deletion locus by fine scale mapping

Although the sequences flanking the breakpoint in the E14TG2a cell line (and subclones) and *Hprt1*^{b-m3} mice are characterized [27], the exact breakpoint has never been defined. We used direct sequence

comparison between WT and *Hprt1*^{b-m3} DNA and fully characterized the 36 kb deletion [10], to determine the precise location of the breakpoint, which lies 415 bp after the 3' end of Exon 2 (Fig. 2A). The fine scale mapping of the locus allowed us to design new, more defined primer sets that distinguish between the *Hprt1*^{b-m3} (*b-m3*) and the *Hprt1* WT mouse alleles (Fig. 2B). We have also designed primers that are specific to the *HPRT1*-complementary sequence (*HPRT1*-CS; human-to-mouse) in our *Hprt1* targeting vector backbones (along with the corresponding mouse-specific assay) (Table 2). This *HPRT1*-CS assay only amplifies a 'complemented' product when the *Hprt1* locus is complemented by a homologous targeting event. These assays consistently and clearly amplify in our ESCs, knock-in (KI) clones, and germline mice. The presence of both the *Hprt1* WT and *HPRT1*-CS alleles, but not the *b-m3* and 'WT @ CS' alleles, in our KI clones indicates that the *HPRT1*-CS has corrected the deletion and integrated correctly at the *Hprt1* locus (Fig. 2C). However, it is important to note that the *Hprt1* WT assay at the breakpoint cannot distinguish between WT mouse *Hprt1* and a complemented *Hprt1* after a targeting event, whereas our *HPRT1*-CS assay can, and neither of these assays can determine copy number, nor can they distinguish between a combination of a correct targeting and a random integrant elsewhere in the genome, or a scrambled targeting event at the *Hprt1* locus.

High germline competency obtained with new B6129F1 hybrid *Hprt1*^{b-m3} ESC lines

Thirty-eight new hybrid *Hprt1*^{b-m3} ESC lines were established utilizing the B6.129P2-*Hprt1*^{b-m3} (B6-*Hprt1*^{b-m3}) and B6.129S4-*Gt(ROSA)26Sor*^{tm1Sor/J} (129-*ROSA26*) mouse strains, and six of these (mEMS1202, mEMS1205, and mEMS1217 (*Gt(ROSA)26Sor*^{+/+}) and mEMS1204, mEMS1213, and mEMS1218 (*Gt(ROSA)26Sor*^{tm1Sor/+})) were chosen for initial characterization. mEMS1204 (B6129F1-*Gt(ROSA)26Sor*^{tm1Sor/+}, *Hprt1*^{b-m3/Y}), was expanded to compare its germline potential with the current standard *Hprt1* deficient cell line, E14TG2a. Both cell lines were microinjected and generated chimeras, which were then bred to allow for direct comparison of germline competency. Microinjection of mEMS1204 into 98 B6(Cg)-*Tyr*^{c-2/J} (B6-Alb) blastocysts demonstrated a high level of sex-reversal in the resultant chimeras (24 male: 4 female, $P < 0.001$ (Fig. 3A)). Twenty-one of the male chimeras (8.5–65% coat color chimerism) were bred to B6-Alb females, 17 (81%) of them producing an average of 6 germline pups/litter (Figs. 3B and 4), and 13 of these 17 male chimeras gave 100% germline pups (average 6 pups/litter). In all cases, germline progeny were identified by the presence of the *Tyr*⁺ (tyrosinase WT) coat color allele in combination with the dominant *A*^w (white bellied agouti) or recessive *a* (nonagouti) coat color alleles

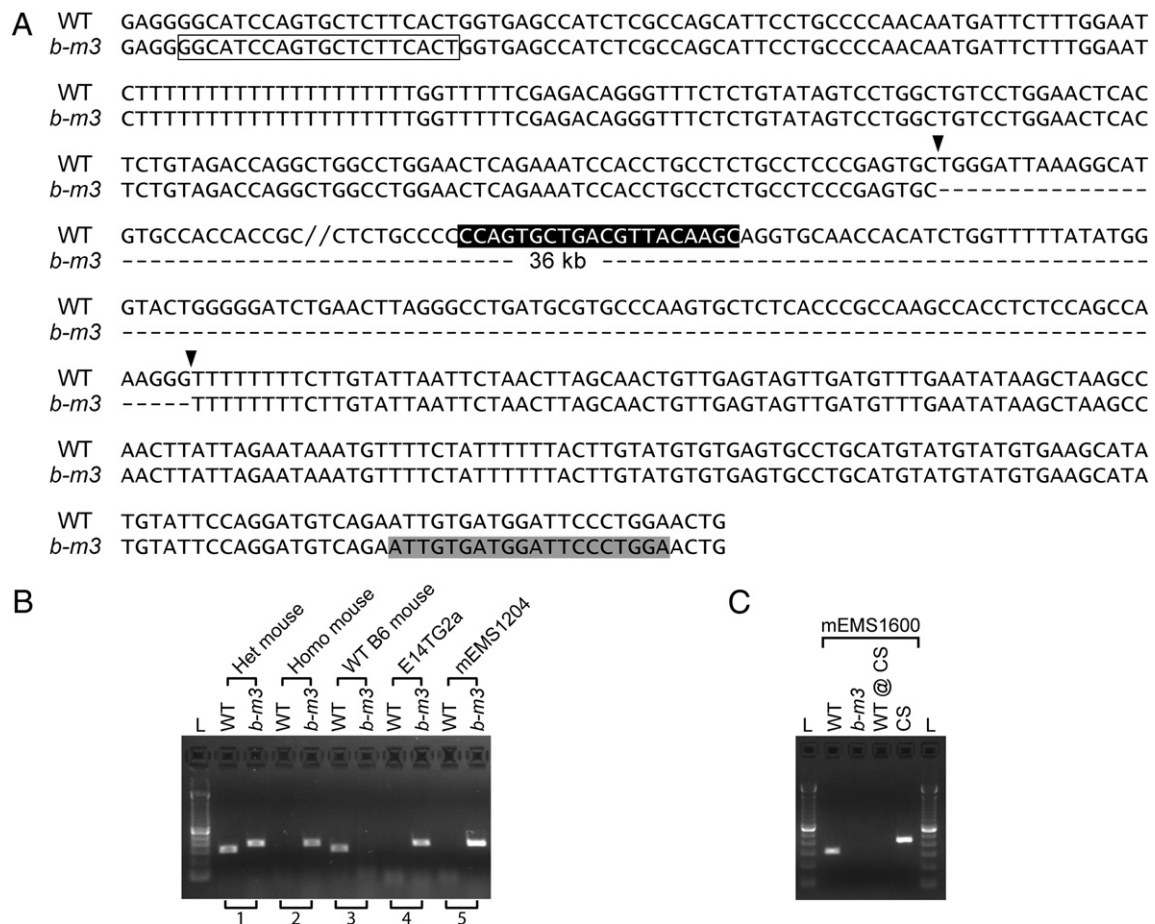


Fig. 2. Delineation of the precise location of the breakpoint at the *Hprt1*^{b-m3} locus. (A) Comparison of the wild-type (WT) and *Hprt1*^{b-m3} (*b-m3*) sequences defines the break point at the *Hprt1* locus. Arrowheads signify breakpoint location. Using the newly defined breakpoint sequence, more specific PCR assays for the WT and *b-m3* alleles were designed. White box denotes oEMS2240 (*b-m3* forward primer); Black box denotes oEMS2238 (WT forward primer); Grey box denotes oEMS2236 (located on antisense strand) (common reverse primer). (B) New *Hprt1* assay distinguishes between the WT and *b-m3* alleles in mice and ESCs. (1) *Hprt1*^{b-m3/+} heterozygous (Het) mouse shows both alleles; (2) *Hprt1*^{b-m3} homozygous (Homo) mouse shows only the *b-m3* allele; (3) C57BL/6J mouse shows only the WT allele; (4) E14TG2a ESCs show only the *b-m3* allele; (5) mEMS1204 ESCs show only the *b-m3* allele. L, 100 bp ladder. (C) The *HPRT1*-CS (CS) assay in combination with the *Hprt1* WT assay indicates proper homologous recombination at the *Hprt1* locus. mEMS1600 ESC clone DNA shows only the *Hprt1* WT allele and not the *b-m3* allele indicating a complemented *Hprt1* locus. The 'WT @ CS' allele does not amplify whereas the CS allele amplifies indicating the presence of the human-to-mouse DNA from the vector backbone in the mEMS1600 ESC clone DNA. L, 100 bp ladder.

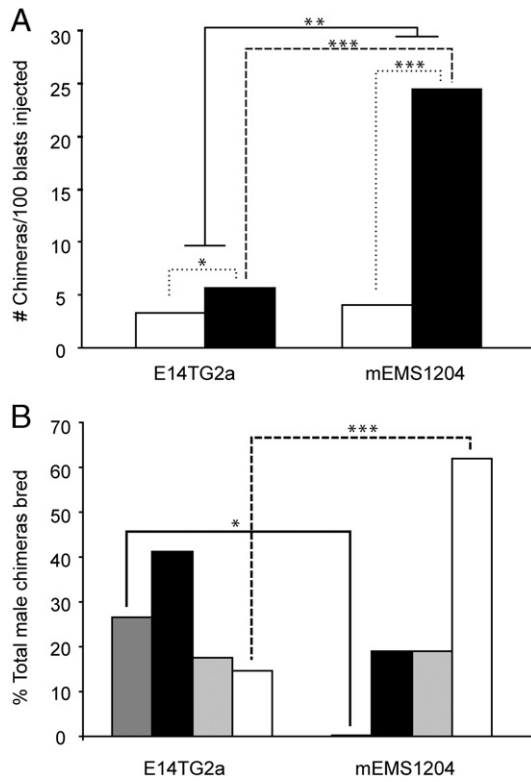


Fig. 3. New hybrid ESC line, mEMS1204, is superior to E14TG2a. (A) Injection of mEMS1204 ESCs results in significantly more chimeras born/total blastocysts injected compared to E14TG2a (solid line, $**P < 0.005$; E14TG2a: 57 chimeras/636 blastocysts, mEMS1204: 28 chimeras/98 blastocysts). Of the total chimeras born/total blastocysts injected, mEMS1204 ESC injections also produced significantly more male chimeras (dashed line, $***P < 0.001$). mEMS1204 ESCs also show extensive sex reversal in chimeric offspring compared to E14TG2a (dotted lines, mEMS1204, $***P < 0.001$; E14TG2a, $*P < 0.05$). Data shown is normalized to 100 blastocysts. White = female chimeras, black = male chimeras. (B) Male chimeras derived from mEMS1204 demonstrate a significantly higher rate of fertility and germline competence than those derived from E14TG2a. None of the mEMS1204 male chimeras were sterile compared to 26.5% sterility observed in E14TG2a chimeras ($*P < 0.05$; dark grey bars) and over 60% of mEMS1204 chimeras demonstrated 100% germline competence compared to only 14.7% of E14TG2a chimeras ($***P < 0.001$; white bars). Both cell lines generated males that were fertile but non-germline (black bars; 41% E14TG2a vs. 19% mEMS1204), and males that were less than 100% germline (light grey bars; 17.6% E14TG2a vs. 19% mEMS1204).

resulting in progeny that appeared brown with a cream belly or black, respectively. Non-germline progeny, homozygous for the *Tyr^{c-2j}* (albino 2 Jackson) coat color allele of the donor B6-Alb strain, appeared white. Microinjection of the two other established B6129F1-*Gt(ROSA)26Sor^{tm1Sor/+}* ESC lines (mEMS1213 and mEMS1218) gave similar results (data not shown). Importantly, we have designed new PCR assay for the *Tyr^{c-2j}* allele, facilitating its removal in subsequent generations of progeny derived from these new ESCs without solely relying on breeding to achieve full congenic status on the B6 background.

Injection of E14TG2a into 636 blastocysts from C57BL/6J (B6) and B6-Alb, demonstrated a very low level of sex-reversal (36 male: 21 female, $P < 0.05$ (Fig. 3A)). Thirty-four of the male chimeras (2–85% coat color chimerism) were bred to B6 or B6-Alb females, 11 (32%) of them producing an average of 3 germline pups/litter (Fig. 3B) and 5 of these 11 male chimeras gave 100% germline pups (average 6 pups/litter). Germline pups from B6 matings were identified by the presence of the dominant *A^w*, resulting in progeny that appeared brown with a cream belly, whereas non-germline progeny, homozygous for the recessive *a* coat color allele of the donor B6 strain, appeared black. Germline progeny from B6-Alb matings were identified by the combination of *A^w* and *Tyr^{c-2j}* (chinchilla) coat

color alleles, resulting in progeny that appear golden, whereas non-germline progeny, homozygous for the *Tyr^{c-2j}* coat color allele of the donor B6-Alb strain, appeared white.

It is well known that hybrid ESC lines have the potential to successfully produce ESC-derived mice through co-culture/complementation [28–30], whereas inbred ESC lines such as E14TG2a lack this ability [21]. We tested the diploid co-culture ability of untargeted and multiple knock-in mEMS1204 ESC lines and have successfully derived germline competent mouse strains using the method of Lee et al. [30] (data not shown).

Widespread expression in mEMS1600 strain validates new tools for *Hprt1* targeting

To confirm the effectiveness of our new tools, we processed the brains of post-natal day 14 (P14) germline N3 (third generation backcross to C57BL/6J) mice from our B6.129P2-*Hprt1^{tm2(CAG-EGFPm1600)/Ems}* (mEMS1600) CAG strain and examined them for EGFP expression (Fig. 5). We compared the expression of mEMS1600 to that of the B6-(CAG-EGFP)10sb strain, a random insertion multiple copy CAG strain (M. Okabe, Genome Information Research Center, Research Institute for Microbial Diseases, Osaka University, Osaka, Japan, March 26, 2008, pers. comm.). The EGFP reporter can be observed under confocal fluorescence with illumination using FITC (fluorescein isothiocyanate) excitation/emission filter sets (Bio-Rad, Hercules, CA). As predicted, all brain regions examined in the mEMS1600 strain showed widespread expression of EGFP under the control of the CAG promoter (Fig. 5A). Strikingly, the EGL (external granular layer) in the mEMS1600 mice showed very high EGFP expression, a unique expression pattern for this CAG strain. Additionally, the mEMS1600 strain does not show extensive expression of EGFP in blood vessels that is seen in the B6-(CAG-EGFP)10sb strain (Fig. 5C). The observed fluorescence intensity seen in mEMS1600 brains is substantially less than that seen in age matched B6-(CAG-EGFP)10sb brains. These intensity differences are likely due to the fact that the mEMS1600 CAG-EGFP expression construct is present in the genome as a single copy, in contrast with the random insertion multiple copy transgene in the B6-(CAG-EGFP)10sb CAG strain.

Discussion

We have designed a set of molecular tools which facilitate single copy, site-specific knock-in (KI) targeting to the *Hprt1* locus. The new pEMS1306 and pEMS1307 vectors in conjunction with the new



Fig. 4. Germline competent chimera derived from mEMS1204 ESCs. Chimeras bred to B6-Alb females can produce 3 colors of N1 progeny. N1 germline progeny will carry the *Tyr⁺* (tyrosinase wild type) with *A^w* (white bellied agouti) or *a* (nonagouti) alleles making them appear brown with a cream belly, or black, respectively. Non-germline progeny will be homozygous for the *Tyr^{c-2j}* (albino 2 Jackson) allele making them appear white.

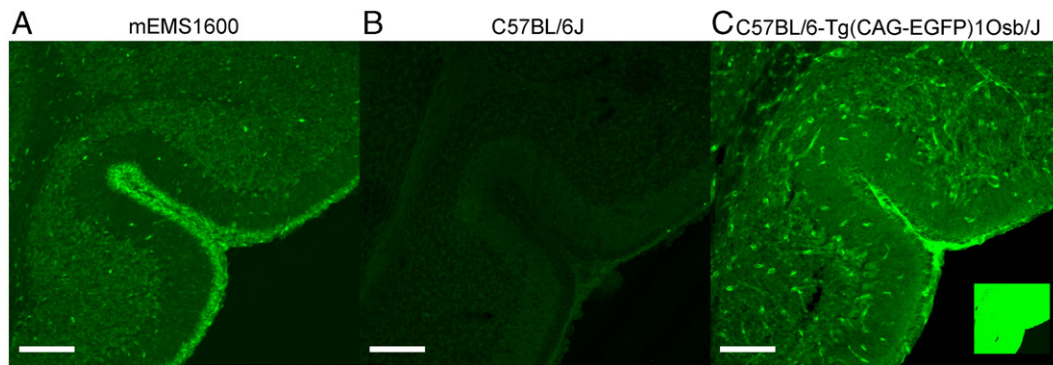


Fig. 5. Widespread expression of EGFP driven by CAG validates the new *Hprt1* tool set. Confocal images from the cerebellum of (A) mEMS1600 (CAG driving EGFP) P14 germline N3, demonstrates direct EGFP fluorescence, with high EGFP expression seen in the EGL, and very little in the blood vessels; (B) an age matched C57BL/6J demonstrates the level of background green fluorescence in the green channel in absence of EGFP expression; and (C) an age matched C57BL/6-Tg(CAG-EGFP)10sb heterozygote (random insertion, multi-copy) demonstrates EGFP expression driven by a similar CAG promoter in the context of a traditional transgenic animal, showing high levels of EGFP expression throughout the brain, especially in the blood vessels. (A) and (B) images were captured using 100% laser intensity and optimal gain settings and (C) was captured at 30% the laser intensity and 50–60% the gain. The inset in (C) shows this section captured at 100% laser intensity and optimal gain settings. Scale bar = 100 μ m.

mEMS1204 hybrid ESC line have enabled us to generate new EGFP-expressing *Hprt1* KI mice which express the EGFP reporter gene. We are currently using this new *Hprt1* tool set as part of the Pleiades Promoter Project to test 250 human MiniPromoter KI constructs at the *Hprt1* locus (<http://www.pleiades.org>). These MiniPromoters are from a set of 70 genes that are expressed in spatially and temporally defined areas of the brain, which have an association with human disease. This new *Hprt1* tool set has proven to be highly efficient, straightforward, and has advanced the existing technologies.

Our purpose in deriving single-copy KI is to recapitulate the physiological levels of gene expression, but we are currently examining ways in which we will be able to increase the levels of EGFP expression in our vectors. One method for increasing the expression of our EGFP reporter would be the addition of an intron [31,32] into the vector backbone, thus splicing would occur regardless of the promoter insert. This method has been shown to increase the transcriptional efficiency of reporter genes 10 to 100 fold [33,34]. The use of insulators in expression vectors is another possible method. For example, Ciavatta et al. [35] have shown that using DNA insulators during targeting to the *Hprt1* locus enhanced expression of the targeted transgene, showing promise for the increased effectiveness of our *Hprt1* tool set.

It is well known that hybrid ESC lines are capable of producing viable embryos using diploid and tetraploid complementation/aggregation technologies [21,28,29,36] whereas existing inbred ESC lines (e.g. E14TG2a) are not [21]. This phenomenon is attributed to the fact that deleterious homozygous genes and/or modifiers of gene expression are made heterozygous, the phenomenon of ‘hybrid vigor’. We have successfully tested the ability of mEMS1204, a new hybrid ESC line, to derive chimeras through diploid aggregation, and predict this cell line will be able to do the same with tetraploid methodologies.

Traditionally, the host blastocyst for microinjection is C57BL/6 (B6) [37] as the majority of standard ESC lines are derived from 129 substrains. These 129-derived ESC lines carry the dominant *A* (agouti) coat color allele at the nonagouti (*a*) locus and will generate germline progeny that appear brown, and non-germline progeny, derived from the host blastocyst, which appear black. Since mEMS1204 ESCs are heterozygous (A^w/a) at the non-agouti locus, using the traditional B6 (*a/a*) host blastocysts would result in half the germline progeny and all the non-germline progeny being homozygous for the non-agouti (*a/a*) coat color allele, and therefore black. This would necessitate all black progeny being genotyped for the transgene, which would be time consuming. These current ESC series are therefore limited to injections using the albino strain B6(Cg)-*Tyr^{c-2j}/J* (B6-Alb) as the blastocyst donor. Resultant germline progeny can then be easily

identified as they will carry the wild-type allele at the tyrosinase (*Tyr⁺*) locus, in combination with the A^w or *a* alleles, making them appear brown with a cream belly or black, respectively, whereas non-germline progeny will be homozygous for the albino allele at *Tyr* (*Tyr^{c-2j}*) and appear white. We are currently developing new hybrid ESC lines which will utilize the agouti C57BL/6J- A^w/J (JAX Stock#000051; B6-Ag) mouse strain, which is homozygous for the dominant A^w/J (white bellied agouti Jackson) coat color allele. ESCs derived from a cross between the B6-Ag and 129S1/SvImJ strains will carry the agouti alleles from both parental strains ($A^w/J/A^w$) and will therefore be able to make use of both the B6-Alb (*a/a*, *Tyr^{c-2j}/Tyr^{c-2j}*) and classic C57BL/6 (*a/a*, *Tyr⁺/Tyr⁺*) strains as host blastocysts. When crossed back to the host strain(s), all the germline progeny generated will be heterozygous for one of the dominant *A* alleles and the *Tyr⁺* allele from the ESCs, and appear brown with a cream belly, whereas non-germline progeny will be black (*a/a*, *Tyr⁺/Tyr⁺* from B6) or white (*a/a*, *Tyr^{c-2j}/Tyr^{c-2j}* from B6-Alb).

We have shown that our newly developed *Hprt1* tool set is a valuable addition to the existing technologies for integration of transgenes into the genome. Our tools facilitate site-specific, single-copy knock-in of an EGFP reporter driven by CAG but also have the flexibility to examine other promoters or genes of interest. Our tools provide a straightforward, efficient alternative to random insertion transgenics.

Materials and methods

Targeting vectors and constructs

Construction of the two targeting vectors pEMS1306 and pEMS1307 (Fig. 1) made use of the pJDH8A/246b I-SceI plasmid [10] as the source of *Hprt1* homology regions required for docking at the mouse *Hprt1* locus. Prior to the use of the pJDH8A/246b I-SceI plasmid [10] the 3' *loxP* site was removed completely and the 5' *loxP* site was mutated by removal of the middle 14 bp (5'-ATGTATGCTATACG-3') sequence using a site-directed mutation approach. Primers loxPmut_P1_L_Kpn1 and loxPmut_P1_R were used to generate PCR product 1 (Table 1). Primers loxPmut_P2_L and loxPmut_P2_R_EcoRI generated PCR product 2. Primer loxPmut_P1_L_Kpn1 is tailed with a KpnI restriction end, primer loxPmut_P2_EcoRI is tailed with an EcoRI end, and primer loxPmut_P1_R is tailed with a 20 bp sequence homologous to the first 20 bp of PCR product 2. PCR products 1 and 2 were used as template in a third PCR reaction to produce the final fusion PCR product 3, a 3397 bp segment with KpnI and EcoRI restriction ends, a single mutated *loxP* site, and no second *loxP* site. The original pJDH8A/246b I-SceI was digested with KpnI and EcoRI to

Table 1
Mutational and amplification primer sequences and assays

Primer name	Primer sequence (5'–3')	Assay
loxPmut_P1_L_Kpn1	GGTACCTCATTGTCAAGACCAG	pJDH8A/246b I-SceI loxP mutation
loxPmut_P1_R	ATTAAGGGTTCGGATCTCA	pJDH8A/246b I-SceI loxP mutation
loxPmut_P2_L	TAGGATCCGGAACCCCTAATAATACTAAGTATTAGGTCCTC	pJDH8A/246b I-SceI loxP mutation
loxPmut_P2_R_EcoRI	GAATTCATTAAGGGTTATTGAATATGA	pJDH8A/246b I-SceI loxP mutation
IV_CAG_F	GAGCTCTGCAGCGCTACATAACT	PCR amplify CAG from pDRIVE-CAG, SacI tailed
IV_CAG_R	ACGCGTGGTGAAGCTACTGTACA	PCR amplify CAG from pDRIVE-CAG, MluI tailed

remove a 3497 bp segment which was replaced by the 3397 bp PCR product 3. The correct assembly for the modification was verified by sequencing, and the new plasmid was called pJDH8A_modlox.

Two different segments of DNA each containing their respective vector elements for pEMS1306 and pEMS1307 were directly synthesized at Genent (Germany) and designed with flanking EcoRI restriction ends for subcloning into the EcoRI linearized pJDH8A_modlox plasmid. The pEMS1306 segment is 1150 bp and includes a multiple cloning site (MCS) that contains SacI, AvrII, MluI, and two octamer restriction enzyme sites, FseI and Ascl. These restriction site sequences can then be incorporated into PCR primers for subcloning fragments into our vectors. The restriction sites were screened against the vector to ensure that they were unique. A Kozak consensus translation initiation site and enhanced green fluorescent protein (EGFP) sequence from pEGFP-N3 (Clontech/BD Biosciences, Mississauga, ON) were added downstream, and the EGFP stop codon was mutated by altering TAA to TTA. Immediately downstream of EGFP is an in-frame 36 bp tetracysteine residue sequence (5'-FLNCCPGCCMEP-3') [22] followed by three copies of an in-frame nuclear localization sequence (NLS), obtained from pACGFP1-Nuc (Clontech, Mountain View, CA). A TAA stop codon was added to the 3' end of the NLS resulting in an EGFP-tetracysteine-NLS fusion protein when expressed. On the 5' end of the EGFP-tetracysteine-NLS sequence is a 34 bp F5 mutant *FRT* sequence and on the 3' end is a 34 bp wild-type (WT) *FRT* sequence. An SV40 early mRNA polyadenylation signal from pEGFP-N3 was included downstream of the *FRT* flanked EGFP-tetracysteine-NLS fusion protein. The pEMS1307 segment was identical to pEMS1306 with the exception that one additional 14 bp (5'-GAAGTTCCTATTCC-3') segment was added to the 5' ends of both *FRT* sites creating full *FRT* (*FFRT*) sites compared to the minimal *FRT* (*MFRT*) sites featured in pEMS1306. Once the synthesized pEMS1306 and pEMS1307 segments were available, each EcoRI tailed segment was subcloned into an EcoRI linearized pJDH8A_modlox plasmid. Each vector was sequence verified using a transposon mediated shotgun approach [38].

The human cytomegalovirus immediate-early enhancer/modified chicken beta-actin (CAG) promoter was directionally cloned into the SacI/MluI digested pEMS1306 and pEMS1307 targeting vectors generating the pEMS1157 and pEMS1277 constructs, respectively. The 1627 bp CAG product was generated from the vector pDRIVE-CAG (Invivogen, San Diego, CA) by PCR amplification using the SacI and MluI tailed PCR primers IV_CAG_F and IV_CAG_R, respectively. Importantly, all our vectors contain a unique I-SceI restriction site for linearization prior to electroporation into ESCs.

Animals and husbandry

B6.129P2-*Hprt1*^{b-m3}/J, abbreviated here as B6-*Hprt1*^{b-m3} (JAX Stock#002171), B6.129S4-*Gt(Rosa)26Sor^{tm1Sor}*/J, abbreviated here as 129-*ROSA26* (JAX Stock#003474), B6(Cg)-*Tyr^{c-2j}*/J, abbreviated here as B6-Alb (JAX Stock#000058), C57BL/6-Tg(CAG-EGFP)10sb/J, abbreviated here as B6-(CAG-EGFP)10sb (JAX Stock#003291), C57BL/6J-*A^{w-j}*/J, abbreviated here as B6-Ag (JAX Stock#000051), C57BL/6J, abbreviated here as B6 (JAX Stock#000664) and 129S1/SvImj, abbreviated here as 129 (JAX Stock#002448) mice were obtained from The Jackson

Laboratory, Bar Harbor, ME, and CD-1(ICR) (Charles River Stock#022) mice were obtained from Charles River, Wilmington, MA and maintained at the Centre for Molecular Medicine and Therapeutics (CMMT). All mice were maintained in the pathogen-free CMMT animal facility on a 6 am–6 pm light cycle, 20±2 °C with 50±5% relative humidity and had food and water *ad libitum*. All procedures involving animals were in accordance with the Canadian Council on Animal Care (CCAC) and UBC Animal Care Committee (ACC) (Protocol# A05-1258 and A05-1748).

Derivation of mEMS1204 embryonic stem cells

Blastocysts were obtained from natural mating of B6-*Hprt1*^{b-m3} females to 129-*ROSA26* males at 3.5 dpc (days post-coital). Blastocysts were flushed from uterine horns as per Hogan et al. [37], cultured in EmbryoMax[®] KSOM with 1/2 Amino Acids, Glucose and Phenol Red (Cat#MR-121, Millipore/Chemicon, Temecula, CA) for 3–5 h, and then transferred onto mitomycin C (mitC; Cat#M4287, Sigma-Aldrich, Oakville, ON) mitotically inactivated B6-*Hprt1*^{b-m3}, B6129F1, or 129 mouse embryonic feeders (MEFs) derived from 13.5-dpc embryos [39] in 96-well plates containing KSR-ESC media (Knockout[™] D-MEM (Cat#10829-018, Invitrogen, Burlington, ON) with 2 mM L-glutamine (Cat#25030-081, Invitrogen, Burlington, ON), 0.1 mM MEM nonessential amino acid solution (Cat#11140-050, Invitrogen, Burlington, ON), 1000 U/ml ESGRO[®] (LIF) (Cat#ESG1107, Millipore/Chemicon, Temecula, CA), and 16% Knockout[™] Serum Replacement (Cat#10828-028, Invitrogen, Burlington, ON)) (MEF media was replaced 3–5 h prior to transfer). Blastocysts were cultured as per Cheng et al. [40] with the following modifications: cells were cultured for 7–9 days in KSR-ESC media with minimal disturbance (checked on day 2 to determine if the blastocysts had 'hatched' out of the zona pellucida) and no media changes. Blastocysts which hatched and had a well developed ICM (inner cell mass) were treated with 20 µl 0.25% trypsin-EDTA (Cat#25200-072, Invitrogen, Burlington, ON) for 5 min at 37 °C, triturated with a 200 µl pipetman, inactivated with 30 µl 0.5 mg/ml soybean trypsin inhibitor (Cat#17075-029, Invitrogen, Burlington, ON), and brought up to 200 µl with KSR-ESC media, then transferred individually to a 24-well MEF plate containing 1800 µl KSR-ESC media, for a total volume of 2 ml. Beginning 4 days later, KSR-ESC media was replaced with FBS-ESC media (DMEM (Cat#11960-069, Invitrogen, Burlington, ON) with 2 mM L-glutamine (Cat#25030-081, Invitrogen, Burlington, ON), 0.1 mM MEM nonessential amino acid solution (Cat#11140-050, Invitrogen, Burlington, ON), 1000 U/ml ESGRO[®] (LIF) (Cat#ESG1107, Millipore/Chemicon, Temecula, CA), 16% ES Cell Qualified fetal bovine serum (FBS, Cat#16141-079, Invitrogen, Burlington, ON), and 0.01% β-mercaptoethanol (Cat#M-7522, Sigma-Aldrich, Oakville, ON)) in 25%, 50%, 75% proportions (respectively) to adapt the cells to FBS containing media. On day 7 the cells were trypsinized to one well of a 24-well plate containing 1 ml of 100% FBS-ESC media, with daily media replacement. Once confluent, wells containing ESC colonies were expanded to 3×24-wells (with MEFs), then passaged to 3×24- (with MEFs) and 3×12-wells (plastic – no MEFs). Once confluent, the 3×24-wells were combined, aliquoted (3 vials), and frozen in ESC-freeze media (50% FBS, 40% FBS-ESC media, 10% DMSO (Cat#D-2650, Sigma-Aldrich, Oakville, ON)), and the 3×12-

wells treated with lysis buffer (Cat#PR-A2361, Fisher Scientific, Ottawa, ON), mixed and aliquoted for future DNA analysis. Cultures were genotyped for X and Y Chromosomes [41], *Gt(ROSA)26Sor^{tm1Sor}* and WT alleles (http://jaxmice.jax.org/pub/cgi/protocols/protocols.sh?objtype=protocol&protocol_id=433, The Jackson Laboratory, Bar Harbor, ME), and *Hprt1^{b-m3}* and WT alleles as listed in Table 2. B6129F1-*Gt(ROSA)26Sor^{tm1Sor}/+*, *Hprt1^{b-m3}/Y* and B6129F1-*Gt(ROSA)26Sor⁺/+*, *Hprt1^{b-m3}/Y* cell lines were identified.

Knock-in at the *Hprt1* locus

Plasmid DNA was purified with the Qiagen Maxi Kit (Cat#12163, Qiagen, Mississauga, ON), resuspended in 10:1 Tris-EDTA (TE, pH7.0) buffer, and linearized with I-SceI (Cat#R0694L, New England Biolabs, Pickering, ON). Linearized plasmid DNA was resuspended in 85 μ l of TE (10:0.1) to a final concentration of 187.5 ng/ μ l. mEMS1204 ESCs were grown to confluence on 4–6 T75 flasks of mitC treated *Hprt1^{b-m3}* MEFs in FBS-ESC media. ESCs ($1.7\text{--}2.5 \times 10^7$) in 720 μ l $1 \times$ PBS were added to the linearized DNA and electroporated in a Bio-Rad Genepulser using a 4 mm electroporation cuvette (Cat#165-2081EDU, Bio-Rad, Mississauga, ON), at 240 V, 50 μ F, 6–10 ms pulse, immediately resuspended in a total volume of 5 ml of FBS-ESC media and plated onto 5×100 mm dishes of mitC B6129F1 WT MEFs in a total volume of 12 ml/100 mm dish. 24–36 h post-electroporation, correctly targeted homologous recombinants were selected for using HAT media (FBS-ESC media containing $1 \times$ HAT ((0.1 mM sodium hypoxanthine, 0.4 mM aminopterin, 0.16 mM thymidine), Cat#21060-017, Invitrogen, Burlington, ON). HAT media was changed every day for the first 3 days, and then every 3rd day thereafter, for up to 10 days. Individual colonies were counted and, typically, no more than 2 isolated colonies were picked per 100 mm dish to optimize for independent homologous recombination events. These colonies were expanded under standard protocols for verification of the desired recombination event.

Purification and PCR analyses of genomic DNA

ESC clone DNA was purified using the Promega Wizard SV Genomic DNA Purification System (Cat#PR-A2361, Fisher Scientific, Ottawa, ON) with the following modifications: the final elution volume varied from 50 μ l run through the column twice, or, 100 μ l or 250 μ l run through once, resulting in approximately 100 ng/ μ l of sample DNA. Tissue samples were digested overnight at 55 °C in 200 μ l of tissue homogenization buffer (THB) (50 mM KCl (Cat#BP366-500, Fisher Scientific, Ottawa, ON), 10 mM Tris-HCl (pH 8.3) (Cat#PR-H5121, Fisher Scientific, Ottawa, ON), 2 mM MgCl₂ (Cat#BP214-500, Fisher Scientific, Ottawa, ON), 0.1 mg/ml gelatin (Cat#G7-500, Fisher Scientific, Ottawa, ON), 0.45% IGEPAL CA-630 (Cat#I8896-50ML, Sigma-Aldrich, Oakville, ON), 0.45% Tween 20 (Cat#BP337-500, Fisher Scientific, Ottawa, ON), autoclaved before use) with 120 μ g/ml Proteinase K (ProK, Cat#P2308, Sigma-Aldrich, Oakville, ON), followed

with 10 min at 95 °C to deactivate the ProK, and a brief spin to debris. Each 25 μ l PCR reaction contained: 200 ng DNA, $1 \times$ PCR buffer (Cat#18038-042, Invitrogen, Burlington, ON), 1.5 mM MgCl₂ (Cat#18038-042, Invitrogen, Burlington, ON), 0.02 U/ μ l Taq Polymerase (Cat#18038-042, Invitrogen, Burlington, ON), 0.2 mM dNTP mix (Cat#10297-018, Invitrogen, Burlington, ON) and 0.5 μ M both forward and reverse primers. 5% dimethyl sulfoxide (DMSO, Cat#D-2650, Sigma-Aldrich, Oakville, ON) was also added to the *HPRT1*-CS assay PCR mix. All PCR assays in Table 2 used the following conditions: 94 °C for 3 min, followed by 35 cycles: 94 °C for 1 min, 61 °C for 1 min, 72 °C for 45 s, and a final extension step at 72 °C for 5 min. Samples were run on a 2% agarose gel ($1 \times$ TBE buffer) containing SYBR safe (2.5 μ l/100 ml gel) (Cat#S33102, Invitrogen, Burlington, ON) under standard conditions. Vector NTI (<http://www.invitrogen.com>) software was used to design PCR assays for the different vector constructs. Table 2 lists all primer sequences and PCR assays used for genotyping.

Derivation of knock-in mice

Chimeric mice from untargeted and targeted ESCs were generated by microinjection [37] into B6 (E14TG2a-derived) and B6-Alb (E14TG2a- and mEMS1204-derived) E3.5 blastocysts, or co-culture [30] with diploid ICR E2.5 morula (cultured overnight to the blastocyst stage), followed by implantation into the uterine horns of 2.5 day pseudopregnant ICR females. Chimeras were identified and coat color chimerism determined as outlined below.

Male chimeras derived from the E14TG2a cell lines were mated with B6 or B6-Alb females, and germline transmission was identified in the former case by the transmission of the dominant *A^w* (white bellied agouti) allele, making the progeny appear brown with a cream belly, or in the latter case by the combination of *A^w* and *Tyr^{c-ch}* (chinchilla), making the progeny appear golden. Non-germline progeny from the cross to B6 were homozygous for the recessive *a* (nonagouti) allele and appeared black, whereas non-germline progeny from the cross to B6-Alb were homozygous for the recessive *Tyr^{c-2J}* (albino) allele and appeared white.

Male chimeras derived from the mEMS1204 cell lines were mated with B6-Alb females, and germline transmission identified by the presence of the dominant *Tyr⁺* (tyrosinase wild type) and the *A^w* (white bellied agouti) or *a* (nonagouti) alleles making the progeny appear brown with a cream belly or black, respectively. Non-germline progeny were homozygous for the recessive *Tyr^{c-2J}* (albino 2 Jackson) allele and appear white. All germline female offspring should carry the knock-in (KI) X Chromosome and were mated with B6 males. N2 offspring were analyzed for the presence of the KI allele by PCR.

Determination of coat color chimerism

E14TG2a- and mEMS1204-derived chimeras were identified and level of coat color chimerism determined as follows. E14TG2a ESCs, homozygous for *A^w* and *Tyr^{c-ch}*, as they are derived from the 129/OlaHsd strain [15], will produce chimeras with cream, chinchilla and agouti patches on a black background when injected into B6 blastocysts. The cream patches result from melanocytes and dermis derived solely from the ESCs (*A^w/A^w*, *Tyr^{c-ch}/Tyr^{c-ch}*), whereas chinchilla patches result from ESC-derived (*A^w/A^w*, *Tyr^{c-ch}/Tyr^{c-ch}*) melanocytes and host-derived (*a/a*, *Tyr⁺/Tyr⁺*) dermis. Agouti patches results from the converse, host-derived melanocytes and ESC-derived dermis. However, E14TG2a ESCs when injected into B6-Alb (*a/a*, *Tyr^{c-2J}/Tyr^{c-2J}*) produce chimeras whose coats contain patches of cream and chinchilla on a white background. The cream patches arise when the melanocytes and dermis are derived primarily from the ESCs (*A^w/A^w*, *Tyr^{c-ch}/Tyr^{c-ch}*), whereas the darker chinchilla areas arise from ESC-derived melanocytes and a host-derived dermis.

mEMS1204-derived chimeras were identified and coat color chimerism determined in the same manner. mEMS1204 ESCs,

Table 2
Genotyping assays and PCR primer sequences

Primer name	Primer sequence (5'–3')	Assay
oEMS2240	GGCATCCAGTCTCTTCACT	<i>Hprt1^{b-m3}</i> allele, forward
oEMS2238	CCAGTGTGACGTTACAAGC	<i>Hprt1</i> WT allele, forward
oEMS2236	TCCAGGGAATCCATCAAAAT	<i>Hprt1</i> common primer, reverse
oEMS2502	TCAAAGGGGTGGATGACCG	Tyrosinase 'C' (WT) allele, forward
oEMS2503	TCAAAGGGGTGGATGACCT	Tyrosinase 'c' allele, forward
oEMS2509	CTCATCCCCAGTTAGTTCTCGAAT	Tyrosinase common primer, reverse
oEMS2364	CGGTATCACGAGGCCCTTTC	In vector, common primer, forward
oEMS2668	GCCAAGTAGGAAAGTCCATAAAG	Promoter-containing (CAG), reverse
oEMS2639	TGGCGGACTTGAAGAAGTCGT	Promoterless (EGFP), reverse
oEMS2267	TCAGGCGAACCTCTCGGCTT	<i>HPRT1</i> -CS (CS) allele, forward
oEMS2272	AGATGAGCTTGGTTGCTGGAGTG	'WT @ CS' allele, forward
oEMS2269	TGCTGGACATCCCTACTAACCCA	CS common primer, reverse

heterozygous A^w/a and homozygous for the Tyr^+ (tyrosinase wild type) alleles will produce chimeras with agouti and black patches on a white background when injected into B6-Alb blastocysts. The agouti patches result when both the melanocytes and dermis are derived solely from the ESCs (A^w/a , Tyr^+/Tyr^+), whereas black patches result from ESC-derived melanocytes and host-derived (a/a , Tyr^{c-2j}/Tyr^{c-2j}) dermis.

In order to rank score the chimeras and preferentially select for chimeras derived from the highest possible ESC contribution, yet recognizing that in some cases we would not be able to conclusively identify which cell lineage contributed to the coat color determining cells, overall chimerism was calculated by conservatively assigning values to the various coat color patches, and summing them. For E14TG2a cells injected into B6 hosts, cream areas were scored as 100% ESC-derived, whereas chinchilla and agouti patches were scored as 50% ESC-derived, and in all cases black areas were scored as 0% ESC-derived. mEMS1204 derived chimeras were scored in the same way where agouti was 100%, black was 50%, and white was 0%, even though white patches may have had some undetectable ESC-contribution (in the dermis specifically). For E14TG2a injections into B6-Alb, the cream and chinchilla patches derived on a white background presented difficulty when attempting to estimate overall coat color chimerism. As such, we estimated the percent chimerism based solely on the total chimerism observed when compared to a white mouse, resulting in slightly inflated overall percent chimerism for this small cohort of mice.

Immunohistochemistry and immunofluorescence

Mice were perfused with 4% paraformaldehyde (PFA) as previously described [42]. Whole brains were dissected out and post-perfusion immersion fixed with PFA for 2–3 h at 4 °C. Brains were then transferred to 20% sucrose at 4 °C overnight with gentle shaking. The brains were cryostat sectioned sagittally at 12–14 μ m and mounted on superfrost-plus slides (Cat#12-550-15, ThermoFisher Scientific, Waltham, MA). EGFP expression was detected by direct fluorescence using a BioRad laser scanning confocal microscope (CLSM, BioRad, Hercules, CA). Equivalent fields from individual animals were captured via CLSM using identical laser power and gain settings (Figs. 5A, B), then laser intensity was reduced to 30% and gain settings were decreased by 50–60% to capture the positive control tissue without overexposure (Fig. 5C).

Statistical analyses

Statistics were performed using Chi-square test (Fig. 3A) and Mann–Whitney *U* Test with *Z* adjustment (Fig. 3B). All analyses were accomplished using the Statistica v6.0 program (Statsoft, Tulsa, OK).

Acknowledgments

The authors thank Melissa McConechy and Mauro Castellarin for their technical skills in assembling and preparing the vectors. We also thank Shadi Khorasan-zadeh, Ivana Komljenovic, Betty Palma, Jenna Turner, Jenny Vermeulen, Siaw Wong, and Athena Ypsilanti for their technical skills in tissue culture; Jing Chen, Kelly Chen, Jun Liu, Kristi Hatakka and Jacek Mis for performing the microinjection and co-culture; Sonia Black, Tara Candido, Erin Flynn, Taryn Hearty, Stéphanie Laprise, Flora Liu and Natalie Wong for perfusions and maintenance of the mouse colonies; Bibiana Wong for her technical skills and advice with perfusions; Jason Cheng and Mahsa Amirabbasi for molecular biology support; and Tony Wong for Information Technology and database development and support. We also thank Meifen Lu and Eric Brauer for their histological skills. Lastly, we wish to thank Catherine van Raamsdonk for her expertise and helpful discussion of coat color genetics and Sarah Bronson for providing the pJDH8A/246b I-Secl

Hprt1 targeting plasmid. CNdL holds a CIHR Canada Graduate Scholarships Master's Award. DG holds a Tier 1 Canada Research Chair in Developmental Neurogenetics. RAH is a Michael Smith Foundation for Health Research Scholar. EMS holds a Tier 2 Canada Research Chair in Genetics and Behaviour. This work was funded in part by Genome British Columbia, Genome Canada, UBC Institute of Mental Health, Child and Family Research Institute, UBC Office of the Vice President Research, BC Mental Health and Addiction Services, and GlaxoSmithKline R&D Ltd.

References

- H.F. Farhadi, P. Lepage, R. Forghani, H.C. Friedman, W. Orfali, L. Jasmin, W. Miller, T.J. Hudson, A.C. Peterson, A combinatorial network of evolutionarily conserved myelin basic protein regulatory sequences confers distinct glial-specific phenotypes, *J. Neurosci.* 23 (2003) 10214–10223.
- J.D. Heaney, S.K. Bronson, Artificial chromosome-based transgenes in the study of genome function, *Mamm. Genome* 17 (2006) 791–807.
- K.I. Matthaei, Genetically manipulated mice: a powerful tool with unsuspected caveats, *J. Physiol.* 582 (2007) 481–488.
- G.A. Soliman, R. Ishida-Takahashi, Y. Gong, J.C. Jones, R.L. Leshan, T.L. Saunders, D.C. Fingar, M.G. Myers Jr., A simple qPCR-based method to detect correct insertion of homologous targeting vectors in murine ES cells, *Transgenic Res.* 16 (2007) 665–670.
- A. Oberstein, A. Pare, L. Kaplan, S. Small, Site-specific transgenesis by Cre-mediated recombination in *Drosophila*, *Nat. Methods* 2 (2005) 583–585.
- S.H. Kim, J.C. Moores, D. David, J.G. Respass, D.J. Jolly, T. Friedmann, The organization of the human HPRT gene, *Nucleic Acids Res.* 14 (1986) 3103–3118.
- P.I. Patel, P.E. Framson, C.T. Caskey, A.C. Chinnault, Fine structure of the human hypoxanthine phosphoribosyltransferase gene, *Mol. Cell. Biol.* 6 (1986) 393–403.
- D.G. Sculley, P.A. Dawson, B.T. Emmerson, R.B. Gordon, A review of the molecular basis of hypoxanthine–guanine phosphoribosyltransferase (HPRT) deficiency, *Hum. Genet.* 90 (1992) 195–207.
- J.T. Stout, C.T. Caskey, HPRT: gene structure, expression, and mutation, *Annu. Rev. Genet.* 19 (1985) 127–148.
- J.D. Heaney, A.N. Rettew, S.K. Bronson, Tissue-specific expression of a BAC transgene targeted to the *Hprt* locus in mouse embryonic stem cells, *Genomics* 83 (2004) 1072–1082.
- R.J. Torres, J.G. Puig, Hypoxanthine–guanine phosphoribosyltransferase (HPRT) deficiency: Lesch–Nyhan syndrome, *Orphanet. J. Rare Dis.* 2 (2007) 48.
- S.B. Dunnett, D.J. Sirinathsinghji, R. Heavens, D.C. Rogers, M.R. Kuehn, Monoamine deficiency in a transgenic (*Hprt*⁻) mouse model of Lesch–Nyhan syndrome, *Brain Res.* 501 (1989) 401–406.
- S. Finger, R.P. Heavens, D.J. Sirinathsinghji, M.R. Kuehn, S.B. Dunnett, Behavioral and neurochemical evaluation of a transgenic mouse model of Lesch–Nyhan syndrome, *J. Neurol. Sci.* 86 (1988) 203–213.
- H.A. Jinnah, F.H. Gage, T. Friedmann, Amphetamine-induced behavioral phenotype in a hypoxanthine–guanine phosphoribosyltransferase-deficient mouse model of Lesch–Nyhan syndrome, *Behav. Neurosci.* 105 (1991) 1004–1012.
- M. Hooper, K. Hardy, A. Handyside, S. Hunter, M. Monk, HPRT-deficient (Lesch–Nyhan) mouse embryos derived from germline colonization by cultured cells, *Nature* 326 (1987) 292–295.
- S.K. Bronson, E.G. Plaehn, K.D. Kluckman, J.R. Hagaman, N. Maeda, O. Smithies, Single-copy transgenic mice with chosen-site integration, *Proc. Natl. Acad. Sci. U. S. A.* 93 (1996) 9067–9072.
- T. Doetschman, R.G. Gregg, N. Maeda, M.L. Hooper, D.W. Melton, S. Thompson, O. Smithies, Targeted correction of a mutant *Hprt* gene in mouse embryonic stem cells, *Nature* 330 (1987) 576–578.
- V. Evans, A. Hatzopoulos, W.C. Aird, H.B. Rayburn, R.D. Rosenberg, J.A. Kuivenhoven, Targeting the *Hprt* locus in mice reveals differential regulation of *Tie2* gene expression in the endothelium, *Physiol. Genomics* 2 (2000) 67–75.
- B. Cvetkovic, H.L. Keen, X. Zhang, D. Davis, B. Yang, C.D. Sigmund, Physiological significance of two common haplotypes of human angiotensinogen using gene targeting in the mouse, *Physiol. Genomics* 11 (2002) 253–262.
- B. Cvetkovic, B. Yang, R.A. Williamson, C.D. Sigmund, Appropriate tissue- and cell-specific expression of a single copy human angiotensinogen transgene specifically targeted upstream of the *HPRT* locus by homologous recombination, *J. Biol. Chem.* 275 (2000) 1073–1078.
- R.P. Misra, S.K. Bronson, Q. Xiao, W. Garrison, J. Li, R. Zhao, S.A. Duncan, Generation of single-copy transgenic mouse embryos directly from ES cells by tetraploid embryo complementation, *BMC Biotechnol.* 1 (2001) 12.
- G.M. Galetta, B.N. Giepmans, T.J. Deerinck, W.B. Smith, L. Ngan, J. Llopis, S.R. Adams, R.Y. Tsien, M.H. Ellisman, Golgi twins in late mitosis revealed by genetically encoded tags for live cell imaging and correlated electron microscopy, *Proc. Natl. Acad. Sci. U. S. A.* 103 (2006) 17777–17782.
- T. Schlake, J. Bode, Use of mutated FLP recognition target (FRT) sites for the exchange of expression cassettes at defined chromosomal loci, *Biochemistry* 33 (1994) 12746–12751.
- L.A. Lyznik, J.C. Mitchell, L. Hirayama, T.K. Hodges, Activity of yeast FLP recombinase in maize and rice protoplasts, *Nucleic Acids Res.* 21 (1993) 969–975.
- J. Seibler, J. Bode, Double-reciprocal crossover mediated by FLP-recombinase: a concept and an assay, *Biochemistry* 36 (1997) 1740–1747.
- J. Seibler, D. Schubeler, S. Fiering, M. Groudine, J. Bode, DNA cassette exchange in ES cells mediated by Flp recombinase: an efficient strategy for repeated

- modification of tagged loci by marker-free constructs, *Biochemistry* 37 (1998) 6229–6234.
- [27] C. McEwan, D.W. Melton, A simple genotyping assay for the Hprt null allele in mice produced from the HM-1 and E14TG2a mouse embryonic stem cell lines, *Transgenic Res.* 12 (2003) 519–520.
- [28] G.S. Eakin, A.K. Hadjantonakis, Production of chimeras by aggregation of embryonic stem cells with diploid or tetraploid mouse embryos, *Nat. Protoc.* 1 (2006) 1145–1153.
- [29] A. Nagy, J. Rossant, R. Nagy, W. Abramow-Newerly, J.C. Roder, Derivation of completely cell culture-derived mice from early-passage embryonic stem cells, *Proc. Natl. Acad. Sci. U. S. A.* 90 (1993) 8424–8428.
- [30] K.H. Lee, C.K. Chuang, H.W. Wang, L. Stone, C.H. Chen, C.F. Tu, An alternative simple method for mass production of chimeric embryos by coculturing denuded embryos and embryonic stem cells in Eppendorf vials, *Theriogenology* 67 (2007) 228–237.
- [31] P.E. Habets, A.F. Moorman, D.E. Clout, M.A. van Roon, M. Lingbeek, M. van Lohuizen, M. Campione, V.M. Christoffels, Cooperative action of Tbx2 and Nkx2.5 inhibits ANF expression in the atrioventricular canal: implications for cardiac chamber formation, *Genes Dev.* 16 (2002) 1234–1246.
- [32] I.J. Huijbers, P. Krimpenfort, P. Chomez, M.A. van der Valk, J.Y. Song, E.M. Inderberg-Suso, A.M. Schmitt-Verhulst, A. Berns, B.J. Van den Eynde, An inducible mouse model of melanoma expressing a defined tumor antigen, *Cancer Res.* 66 (2006) 3278–3286.
- [33] H. Le Hir, A. Nott, M.J. Moore, How introns influence and enhance eukaryotic gene expression, *Trends Biochem. Sci.* 28 (2003) 215–220.
- [34] A. Nott, S.H. Meislin, M.J. Moore, A quantitative analysis of intron effects on mammalian gene expression, *RNA* 9 (2003) 607–617.
- [35] D. Ciavatta, S. Kalantry, T. Magnuson, O. Smithies, A DNA insulator prevents repression of a targeted X-linked transgene but not its random or imprinted X inactivation, *Proc. Natl. Acad. Sci. U. S. A.* 103 (2006) 9958–9963.
- [36] K. Eggan, H. Akutsu, J. Loring, L. Jackson-Grusby, M. Klemm, W.M. Rideout III, R. Yanagimachi, R. Jaenisch, Hybrid vigor, fetal overgrowth, and viability of mice derived by nuclear cloning and tetraploid embryo complementation, *Proc. Natl. Acad. Sci. U. S. A.* 98 (2001) 6209–6214.
- [37] B. Hogan, R. Beddington, F. Costantini, E. Lacy, *Manipulating the Mouse Embryo*, Cold Spring Harbor Laboratory Press, Cold Spring Harbor, 1994.
- [38] Y.S. Butterfield, M.A. Marra, J.K. Asano, S.Y. Chan, R. Guin, M.I. Krzywinski, S.S. Lee, K.W. MacDonald, C.A. Mathewson, T.E. Olson, P.K. Pandoh, A.L. Prabhu, A. Schnerch, U. Skalska, D.E. Smailus, J.M. Stott, M.I. Tsai, G.S. Yang, S.D. Zuyderduyn, J.E. Schein, S.J. Jones, An efficient strategy for large-scale high-throughput transposon-mediated sequencing of cDNA clones, *Nucleic Acids Res.* 30 (2002) 2460–2468.
- [39] L. Ponchio, L. Duma, B. Oliviero, N. Gibelli, P. Pedrazzoli, G. Robustelli della Cuna, Mitomycin C as an alternative to irradiation to inhibit the feeder layer growth in long-term culture assays, *Cytotherapy* 2 (2000) 281–286.
- [40] J. Cheng, A. Dutra, A. Takesono, L. Garrett-Beal, P.L. Schwartzberg, Improved generation of C57BL/6J mouse embryonic stem cells in a defined serum-free media, *Genesis* 39 (2004) 100–104.
- [41] S.J. Clapcote, J.C. Roder, Simplex PCR assay for sex determination in mice, *Biotechniques* 38 (2005) 702, 704, 706.
- [42] K.A. Young, M.L. Berry, C.L. Mahaffey, J.R. Saionz, N.L. Hawes, B. Chang, Q.Y. Zheng, R.S. Smith, R.T. Bronson, R.J. Nelson, E.M. Simpson, Fierce: a new mouse deletion of Nr2e1; violent behaviour and ocular abnormalities are background-dependent, *Behav. Brain Res.* 132 (2002) 145–158.